J Mater Sci: Mater Electron (2012) 23:8–13
DOI 10.1007/s10854-011-0381-2

Interface fracture surface energy of sol–gel bonded silicon wafers by three-point bending

B. A. Latella · M. Ignat

Received: 19 January 2011 / Accepted: 15 April 2011 / Published online: 26 April 2011

Abstract To probe the interface of silicon sol–gel bonded wafers we developed *in–situ* micromechanical bending test coupled with optical microscopy. The silicon wafers were bonded together at room temperature using sol–gel silica and dried at 60 °C and sintered at 600 °C. Beam specimens were cut from the bonded wafers, then notched and tested in three-point bending. During bending the crack opening from a notch and the deviation along the interface was observed with an optical microscope. To quantify the interfacial debonding from considering the experimental results, a simple energy balance allows an apparent interfacial fracture surface energy to be determined. Experiments and the determined interfacial surface energies show that the bonding of the silicon wafers depends on the silica sol–gel chemistry and on the temperature of the thermal treatment during the bonding process.

B. A. Latella
Institute of Materials and Engineering Science,
Australian Nuclear Science and Technology Organisation,
Private Mail Bag 1, Menai, NSW 2234, Australia

M. Ignat
Laboratoire de Thermodynamique et de Physico-Chimie
Métallurgique, associé au CNRS, E.N.S.E.E.G, BP 75,
38402 Saint Martin d'Hères, France

M. Ignat
Departamento de Fisica, Facultad de Ciencias Fisicas,
Universidad de Chile, Beauchef 850, Santiago, Chile

B. A. Latella (✉)
Commonwealth Scientific and Industrial Research Organisation,
Waterford, WA 6152, Australia
e-mail: blatella@ozemail.com.au

1 Introduction

Different techniques of silicon wafer bonding have been developed in the microelectronic industry. It is used in the manufacture of integrated circuits, optoelectronic devices and microelectromechanical systems (MEMS). It is a powerful tool for creating layered structures such as silicon on insulator (SOI) devices [1]. Silicon wafers can be bonded with a very thin native oxide layer (hydrophilic surface) or without it (hydrophobic surface, termed Si–Si direct bonding [2]). The wafer bonding process relies on adhesion between the extremely smooth and flat silicon surfaces at ambient temperature and then annealed at high temperature to form strong Si–O–Si bonds [3, 4].

Optimising the adhesive strength of these bonded structures through wafer preparation (i.e. cleaning) and subsequent processing is paramount to achieving a strong and reliable material interface. Reliability in this instance depends on the ability to attach the silicon wafers together in such a way that adequate bonding is achieved so that the main function of the material is not compromised, or fail prematurely under external applied stresses in normal operating conditions, or as a consequence of intrinsic stresses produced during the bonding process, or thermo-elastic stresses, due to the thermal expansion mismatch developed during processing, that may became critical because of the thermal cycling during device operation. Accordingly, as for any microelectronic devices containing thin film structures, controlling the interfacial mechanical properties is an important technological challenge.

For silicon-bonded structures, the properties of the interface have been determined using tensile testing [5], the razor blade wedge technique [6] and by indentation [7]. An extensive review of these tests method used in wafer bonding is given in Ref. [8]. The four-point bend

delamination method [9] was developed to characterise the fracture at interfaces between dissimilar materials and is based on a well-established testing routine that requires simple bar-shaped samples. Three point bending techniques have shown also to provide a quantitative and reproducible measure of interface fracture resistance, in particular for multilayered samples as thick coatings deposited on metal substrates [10–13].

The key advantages of the three point bending method over the indentation and razor blade techniques are the simple configuration and ease of testing. The bending method also allows several samples from a single wafer to be tested. In indentation with a pointed indenter (e.g. Vickers) the impression needs to be made symmetrically across a polished bonded interface with radial cracks extending along the interface [7]. The Vickers indentation is at best only a semi-quantitative technique and is good for comparative checks of bonding for similar interfaces. It is limited to material systems with very thin interlayers and problems have been encountered with strongly bonded wafers [7]. The razor blade method is generally applied to full circular bonded wafers and the blade must induce a straight and uniform linear contact. It is rather delicate to set up an experimental configuration and requires a thin straight and stiff razor.

In this work we consider the issues of measuring the interface surface energy of small silicon bonded beams, extracted from wafer-bonded structures using a straightforward three-point bend test configuration. The goal was to direct the crack generated in notched beams perpendicularly towards an interface to obtain quantitative interfacial fracture energy data, when the cracks deviates along the interface, using a simple energy balance. The results were compared to similar experimental data obtained from indentation and razor blade methods. Implications concerning the interfacial bonding of the silicon wafers using sol–gel derived silica films due to treatment temperature are also discussed.

2 Experimental methods

Sol-gel solutions were prepared by adding a 0.01 M solution of HNO_3 to a solution of tetraethylorthosilicate (TEOS) in ethanol (with an equivalent SiO_2 content of 1 wt%) at pH = 2. A water-to-alkoxide mole ratio of 10 was used and the solutions were filtered using 0.2 μm Teflon membranes then aged for 1 day prior to use. Polished one inch (25.4 mm) silicon wafers (Virginia Semiconductors, average roughness $R_a = 0.2$ nm) of 0.5 mm thickness were pre-treated by degreasing in xylene, followed by the standard RC1/2 cleaning process [14]. A thin layer of sol–gel solution was applied to the cleaned substrates by spin-coating at 5,000 rpm for 2 min. The average surface roughness of the spin coated layers produced was about 0.5 nm. The two coated silicon wafers were then pressed together and the resulting sandwich was dried at 60 °C for 12 h in an oven to allow evaporation of the residual solvent trapped in the sol–gel film. Selected samples were fired in an air atmosphere at 600 °C for 20 h in a muffle furnace. The bonding procedure was conducted in a Class 1,000 clean room to minimise dust contamination. The interlayer film thickness for the 600 °C treated samples was determined from transmission electron microscopy observations. It was found to be about 80 nm [4]. Further details of the wafer bonding process and characteristics of the bonded structures are given elsewhere [4, 15].

Samples with nominal width, thickness and length of 2.5 mm, 1 mm and ≈23 mm, respectively, were sliced from the bonded silicon wafers treated at 60 °C and 600 °C. Typical infrared (IR) transmission images showing the degree of bonding between the wafers are shown in Fig. 1. Fig. 1a indicates that the bonding for the 60 °C treated sample is relatively uniform throughout the entire area whereas Fig. 1b shows that the bonding in part of the sample treated at 600 °C is not good due to the fringe pattern. Based on the IR images, slices were taken from wafers that exhibited good bonding through the entire central region. The top wafer was notched to within about

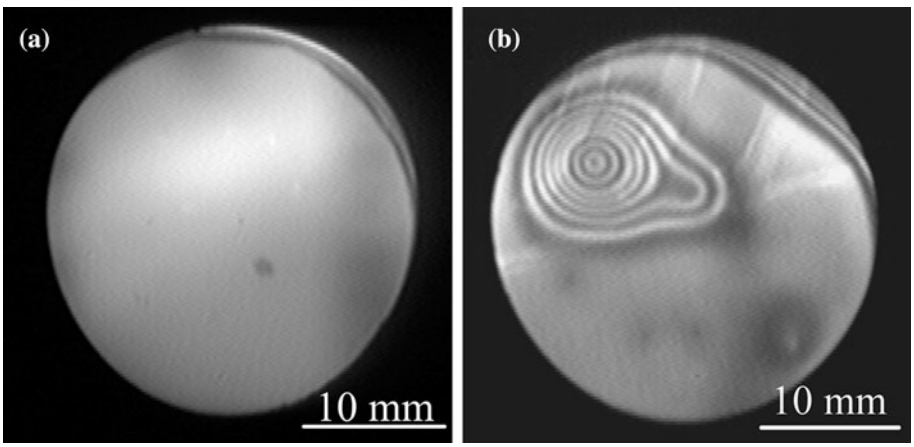

Fig. 1 IR images of 25.4 mm diameter Si-bonded wafers after: **a** 60 °C and **b** 600 °C treatment. Note in **b** the *Newton rings* showing evidence of interfacial debonding

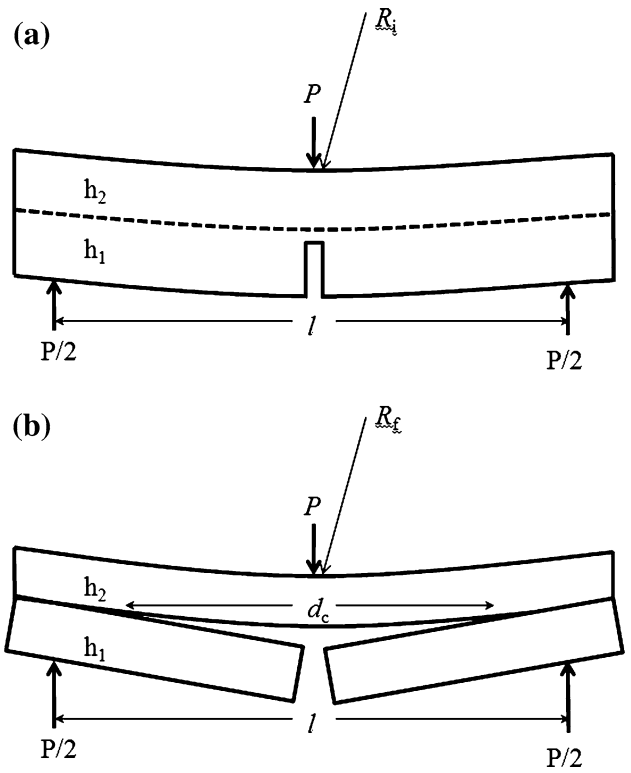

Fig. 2 Schematic representation of the three-point delamination test: **a** during loading before cracking and debonding and **b** at the critical moment where a crack deflects into and propagates along the interface

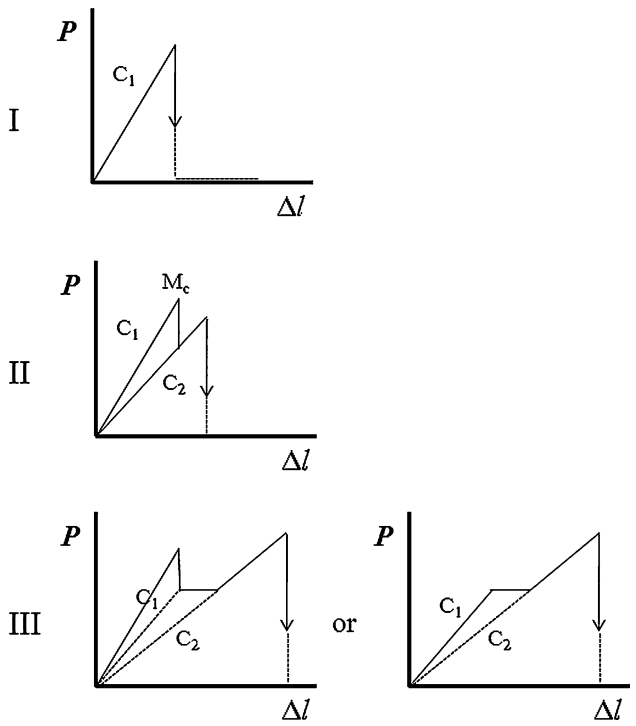

Fig. 3 Three types of bending behaviour based on load–displacement response of bilaminate brittle materials: I—Instantaneous transverse cracking and failure, II—successive transversal fracture and III—stable crack propagation at the interface and final rupture

100 μm of the interface with a thin WC coated blade. A schematic of the crack opening from the notch and the deviation at the interface is shown in Fig. 2. A custom-built high-stiffness small-scale mechanical testing system was used for the experiments as described elsewhere [16]. The samples were placed in the three-point bending device (span = 20 mm) and loaded at a rate of 0.003 mm/s. The jig was positioned under an optical microscope (Zeiss Axioplan) to observe crack initiation and deflection at the interface of the test specimens. Load–displacement data were obtained during testing, from the output of a load cell (20 N capacity) and a displacement transducer. Tests were conducted in a laboratory air environment at ≈24 °C and relative humidity of 45%.

3 Cracking and three-point bending analysis

For a notched bilayered beam consisting of two bonded brittle materials, such as silicon, one can categorise the bending response into three sorts schematically represented in Fig. 3:

I. A catastrophic transversal failure (typical for silicon and brittle materials) on reaching a critical level during the elastic loading.

II. A transversal failure which occurs in two stages: the initial elastic loading unloads partially when the first layer cracks (notched layer); followed by a short elastic reloading of the un-notched layer until this layer breaks.

Both types of behaviour depend strongly on extrinsic parameters such as the geometry of the beams and of the notch, and intrinsically on microstructural defects. They correspond to unstable cracking and failure, driven by the stored elastic energy into the sample during bending. However, for the described notched beams, a third bending behaviour can be detected when the crack opens at the notch but deviates at the interface:

III. The transversal failure occurs after three steps: (i) as for I or II bending responses, an elastic loading increases until reaching a critical load; (ii) then the load remains constant, and corresponds to the deviation of the initial crack from the notch, at the interface (the beam's deflection continues to increase); and (iii) finally the load will increase again, because the interfacial crack stops near the sample's support points, before the final transverse rupture of the uncracked remaining layer.

When this sort of bending behaviour occurs, and experimentally is observed, an apparent interfacial surface

energy value can be determined from the simultaneously recorded load versus displacement data assuming that:

(i) the interfacial crack opening and propagation is stable and occurs at a constant moment (M_c); and
(ii) interfacial debonding occurs without an increase of the global energy stored in the system.

The determination of the interfacial energy starts by considering the geometrical features of the bending system and its evolution. The thicknesses of the lower and upper beams h_1 and h_2, are the same; the width of the composite beam is denoted b (not shown in Fig. 2), l is the distance between the loading points and d_c is the interfacial crack length; R_i and R_f denote the initial and final radius of curvature of the beam, respectively. The flexural rigidity D_i of a beam is:

$$D_i = E_i I_i \tag{1}$$

E_i is the Young Modulus and I_i the first moment of inertia of the beam. In our case i = 1 corresponds to the lower beam and i = 2 to the upper beam. Before the crack activation, both beams are submitted to the same moment and deflection evolution (linear loading), and the two layered composite beam presents a flexural rigidity given by:

$$D_c = E_c I_c = \frac{D_1 D_2}{D_1 + D_2} \tag{2}$$

where the subscript c denotes the composite nature of the bilayer. In our case, both beams are silicon and present the same geometrical characteristics.

When reaching the critical moment M_c, the crack simultaneously opens from the notch and propagates a distance d_c at the interface, between the bending supports, debonding the lower beam from the upper one. Then the radius of curvature of the sample changes from $R_i = E_c I_c / M_c$ to become $R_f = E_2 I_2 / M_c$ (here the subscripts i denote intial and f final).

By considering the general expression of the work (W_o) when a crack opens two free surfaces at the interface:

$$W_o = 2\gamma b d_c \tag{3}$$

where in our case $\gamma = \gamma_i$ is the surface energy at the interface. The global energy balance associated with the previous described process, which assumes stable crack propagation at the interface, will consider the following terms:

- The release of strain energy from notched beam when cracking is:

$$\Delta U_1 = \frac{3D_1}{2}\left(\frac{1}{R_f^2} - \frac{1}{R_i^2}\right) d_c \tag{4}$$

- and the work of the external force applied to the specimen is:

$$\Delta U_2 = \frac{M_c}{2}\left(\frac{1}{R_f} - \frac{1}{R_i}\right) d_c \tag{5}$$

- then the increase of energy in upper beam is:

$$\Delta U_3 = \frac{3D_2}{2}\left(\frac{1}{R_f^2} - \frac{1}{R_i^2}\right) d_c \tag{6}$$

Considering these relations and recalling that the interfacial cracking process occurs at a constant moment, the corresponding energy balance is:

$$\Sigma \Delta U = W_o - \Delta U_1 + \Delta U_2 + \Delta U_3 = 0 \tag{7}$$

Replacing the corresponding relations, we obtain an expression for the interfacial fracture surface energy γ_i:

$$\gamma_i = \frac{M_c^2}{4b}\left[\frac{6}{D_2} - \frac{2}{D_1} - \frac{3D_2}{D_1^2}\right] \tag{8}$$

The critical moment M_c, is given by $M_c = Pl/4$, $D_i = E_i I_i$ and $I_i = b h_i^3/12$ (with i = 1 and 2). In our case for Si–Si bonding both beams are the same, i.e. $D_1 = D_2 = D$ so that equation 8 becomes:

$$\gamma_i = \frac{M_c^2}{4bD} \tag{9}$$

4 Results

Figure 4 shows a specimen bonded at 60 °C prior to the initial stages of loading (Fig. 4a) and then after reaching the critical moment M_c (Fig. 4b). The crack deflection and propagation along the interface is observed. Likewise, Fig. 5 shows a typical loading curve of Si wafers bonded at 60 °C for the three-point bend delamination test. The main feature of the curve (category III behaviour) is the elastic loading of the sample to a point where a crack initiates from the notch and is deflected along the interface (M_c). This corresponds to a load plateau denoted by the thick grey line. Then the crack stops near the loading support points on the sample beam. There is no more interfacial crack opening but further deflection of the system at a larger compliance. Finally the sample fails catastrophically with a sudden load drop. For several samples bonded and sintered at 600 °C the crack did not deflect along the interface but went straight through the lower Si (category I or II) indicative of excellent interfacial bonding.

The results obtained for all specimens tested are plotted in Fig. 6 along with data from similar sol–gel bonded Si wafers using Vickers indentation [7] and Si hydrophilicly bonded at 100 °C and 600 °C and tested using the razor

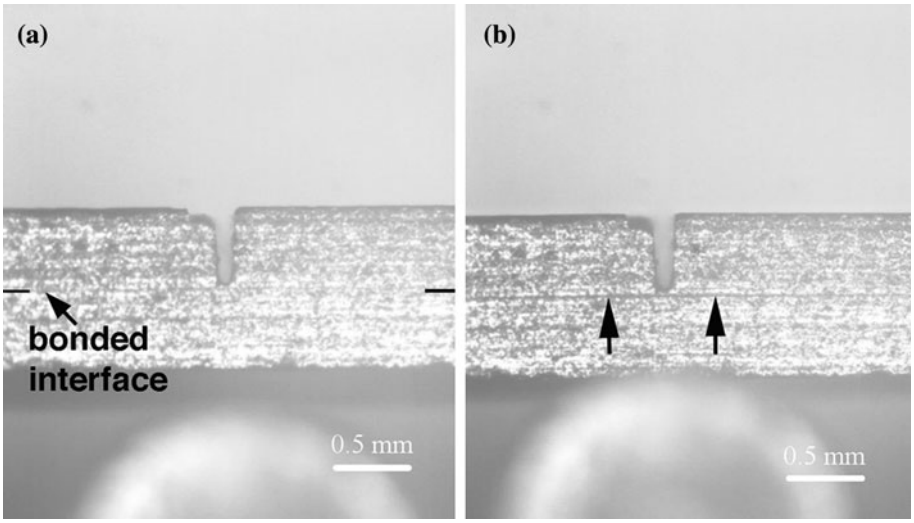

Fig. 4 *In-situ* optical microscopy images showing: **a** specimen prior to loading and **b** deflection of a crack along the interface during the three-point bending

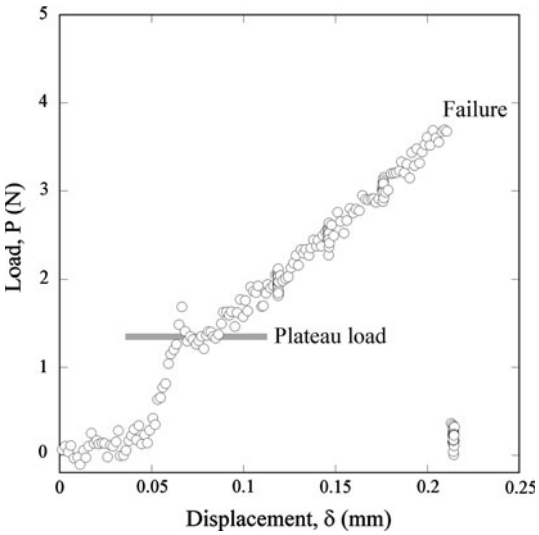

Fig. 5 Typical load–displacement curve for a 60 °C bonded Si wafers. Note the rather small load (P ≈ 1.3 N), corresponding to a constant bending moment, required for crack deflection and propagation along the interface

blade method [17]. The 600 °C treatment yields superior Si wafer bonding over the 60 °C with about a factor of 3 improvement in the apparent interface surface energy from $\gamma_i = 1.4 \pm 0.2$ Jm^{-2} to $\gamma_i = 4.8 \pm 0.6$ Jm^{-2}. This may be compared to the fracture energy of Si, $\gamma = 2.23 \pm 0.24$ Jm^{-2} [7], obtained by Vickers indentation on the same type of wafers used in this study. The apparent interface fracture surface energies determined using the energy balance (Eq. 9) give values that are of the same order but higher in magnitude compared to the indentation and the razor blade technique but the γ trends with respect to treatment temperature are the same in all cases (Fig. 6).

This shows that in bending experiments, and as demonstrated by others [18], the loading angle plays an important role in the energy determination. The energy dissipated for debonding at the interface in bending, occurs from a mixed mode mechanical loading i.e. tension and shear, which accounts for the higher values determined in this work. By contrast the razor blade method, when performed with an optimised experimental set up, is closer to a simple tension loading mode. The tension is applied perpendicular to the interface, so that the determined energy represents the mechanical work to break bonds along an interface, for example breaking chemical bonds and is representative of an intrinsic property of the system. The point loading from a Vickers indenter generates a complex stress field at and around the contact with tensile and shear stress components that decrease with distance from the impression. Nevertheless, as long as the Si wafer bonded system is considered symmetrical (as is the case in ref [7]) the interfacial crack opening can be associated to a tension mode, giving lower interface energy values. The razor blade and indentation data are quite similar although the bonding processes (hydrophilic versus sol–gel) are different as indicated in Fig. 6.

The sol–gel processing involves inorganic polycondensation reactions, which results in the formation of covalent Si–O-Si bonds which become prevalent at higher treatment temperatures. The higher fracture energy of the 600 °C treated specimens is due to a decrease in sol–gel film thickness and increase in the density of the film from 60% to over 90% with removal of organic species that are present in the 60 °C dried film. Thermal analysis shows that pyrolysis of organics groups from the sol–gel solution takes place at around 350 °C [19]. This suggests that the covalent oxygen bridges between the two substrates are much more prevalent in the 600 °C treated specimens and hence the improved interfacial bonding. Similar effects have been observed in direct silicon wafer bonding [6, 17].

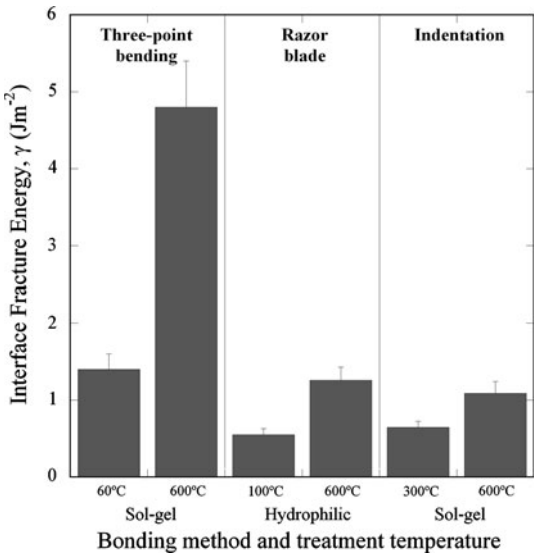

Fig. 6 Comparison of interfacial fracture surface energies of 60 °C and 600 °C bonded Si wafers. Included for comparison are data for hydrophilic bonded Si using razor blade method [17] and sol–gel bonded Si using indentation method [7] at various treatment temperatures. *Error bars* are standard deviations for a minimum of 4 specimens for 3 point bending and from about 20 indents for indentation method

The fracture energies obtained using this energy balance method are similar in magnitude to those obtained from crack opening measurements (razor blade) and direct crack measurements (indentation). Nanoindentation of the sol–gel silica films to ascertain hardness (H) and Young's modulus (E) validates the differences in the adhesion bonding due to the organic species in the films with large differences observed between the low density and high density films. For samples treated at 60 °C $E = 43$ GPa and $H = 2.6$ GPa [20] and for samples treated at 600 °C $E = 65$ GPa and $H = 5$ GPa. The higher E and H values for the 600 °C treated films are related to lower porosity, less organics and a more rigid structure as a result of sintering. These differences have been confirmed in transmission electron microscopy cross-sections of the films in the bonded structures, which show that the 60 °C treated films contain discernible pores and IR spectra show that the 60 °C films contain organics that are no longer present in the 600 °C films but are characterised by Si–O stretching overtones [4, 15].

5 Conclusions

A three-point flexural bend test has been applied to determine the interfacial fracture surface energy of Si wafers bonded using sol–gel technology. Using an energy balance method an equation for determining the interface surface energy was obtained. This simple technique is a suitable means for quantifying the surface energy of brittle–brittle bonded systems. The fracture energy of the 600 °C treated bonded Si wafers was determined to be 4.8 ± 0.6 Jm^{-2} compared to 1.4 ± 0.2 Jm^{-2} for the 60 °C treated samples. The difference in the cracking energy values is due to the morphology of the sol–gel film; after a 60 °C drying, the film is porous and susceptible to crack opening and propagation. Whereas after a 600 °C treatment the film is nearfully densified to a glass-like microstructure, imparting a stronger bond to silicon and improved interfacial fracture resistance.

Acknowledgments Thanks to ANSTO colleagues David Cassidy and Christophe Barbé for fabricating the samples.

References

1. U. Gosele, Q.-Y. Tong, Annu. Rev. Mater. Sci. **28**, 215 (1998)
2. Q.-Y. Tong, U. Gosele, *Semiconductor Wafer Bonding: Science and Technology* (John Wiley & Sons, New York, 1999)
3. A. Plößl, G. Kräuter, Mater. Sci. Eng. Rep. **25**, 1 (1999)
4. C.J. Barbe, D.J. Cassidy, G. Triani et al., Thin Solid Films **488**, 153 (2005)
5. S.N. Farrens, C.E. Hunt, B.E. Roberds, J.K. Smith, J. Electrochem. Soc. **141**, 3225 (1994)
6. W.P. Maszara, G. Goetz, A. Caviglia, J.B. McKitterick, J. Appl. Phys. **64**, 4943 (1988)
7. B.A. Latella, T.W. Nicholls, D.J. Cassidy, C.J. Barbe, G. Triani, Thin Solid Films **411**, 247 (2002)
8. O. Vallin, K. Jonsson, U. Lindberg, Mater. Sci. Eng. Rep. **50**, 109 (2005)
9. P.G. Charalambides, J. Lund, A.G. Evans, R.M. McMeeking, J. Appl. Mech. **56**, 77 (1989)
10. A.J. Phillipps, W.J. Clegg, T.W. Clyne, Acta Metall. **41**, 805 (1993)
11. C. Angelelis, M. Ducarroir, E. Felder, M. Ignat, S. Scordo, Surf. Eng. **13**, 207 (1997)
12. E. Harry, A. Rouzaud, M. Ignat, P. Juliet, Thin Solid Films **332**, 195 (1998)
13. M. Andrieux, M. Ignat, M. Ducarroir, B. Feltz, G. Farges, J. Adhes. Sci. Technol. **16**, 81 (2002)
14. W. Kern, D.A. Puotinen, RCA Rev. **31**, 187 (1970)
15. C.J. Barbe, D.J. Cassidy, G. Triani et al., Thin Solid Films **488**, 160 (2005)
16. M. Ignat, M. Ducarroir, M. Lelogeais, J. Garden, Thin Solid Films **220**, 271 (1992)
17. J. Steinkirchner, T. Martini, M. Reiche, G. Kastner, U. Gosele, Adv. Mater. **7**, 662 (1995)
18. J.W. Hutchinson, Z. Suo, Adv. Appl. Mech. **29**, 64 (1991)
19. C.J. Barbé, D.J. Cassidy, G. Triani et al., J. Sol-Gel. Sci. Technol. **19**, 321 (2000)
20. A.J. Atanacio, B.A. Latella, C.J. Barbe, M.V. Swain, Surf. Coat. Technol. **192**, 354 (2005)